

Reconnection and acoustic emission of quantized vortices in superfluid by the numerical analysis of the Gross-Pitaevskii equation

Shin-ichiro Ogawa¹, Makoto Tsubota¹, Yuji Hattori²

¹*Department of Physics, Osaka City University, Sumiyoshi-Ku, Osaka 588-8585, Japan*

²*Department of Computer Aided Science, Kyusyu Institute of Technology*

Sensui 1-1, Tobata-ku, Kitakyushu 804-8550, Japan

(Received)

We study numerically the reconnection of quantized vortices and the concurrent acoustic emission by the analysis of the Gross-Pitaevskii equation. Two quantized vortices reconnect following the process similar to classical vortices; they approach, twist themselves locally so that they become anti-parallel at the closest place, reconnect and leave separately. The investigation of the motion of the singular lines where the amplitude of the wave function vanishes in the vortex cores confirms that they follow the above scenario by reconnecting at a point. This reconnection is not contradictory to the Kelvin's circulation theorem, because the potential of the superflow field becomes undefined at the reconnection point. When the locally anti-parallel part of the vortices becomes closer than the healing length, it moves with the velocity comparable to the sound velocity, emits the sound waves and leads to the pair annihilation or reconnection; this phenomena is concerned with the Cherenkov resonance. The vortices are broken up to smaller vortex loops through a series of reconnection, eventually disappearing with the acoustic emission. This may correspond to the final stage of the vortex cascade process proposed by Feynman. The change in energy components, such as the quantum, the compressible and incompressible kinetic energy is analyzed for each dynamics. The propagation of the sound waves not only appears in the profile of the amplitude of the wave function but also affects the field of its phase, transforming the quantum energy due to the vortex cores to the kinetic energy of the phase field.

I. INTRODUCTION

The numerical simulations of the quantized vortex dynamics in superfluid are classified into two methods¹. The first is the vortex filament formulation and the second is the numerical analysis of the Gross-Pitaevskii equation(GPE). The former simulation pioneered by Schwarz² is useful for superfluid ⁴He, since the core of quantized vortex is very thin, *i.e.* of the order of atomic size. In this formulation, the motion of vortices is caused by the local and the nonlocal induced velocity fields subject to the Biot-Savart law. When two vortices approach each other within a critical distance, they are assumed to reconnect. The results of this formulation agree excellently with the experimental results of the vortex tangle in superfluid turbulence. However, the significant phenomena concerned with the core structure, such as vortex nucleation, annihilation and reconnection, cannot be described by this formulation.

On the other hand, the analysis of the GPE, which is discussed in this paper, can investigate and analyze the superfluid dynamics including the motion of vortex cores. Koplík and Levine solved numerically the GPE and showed two closed vortices actually reconnected even in an inviscid fluid³. However, they did not show the detail of the reconnection process and the concurrent acoustic emission, *i.e.* the emission of the condensate density waves. This is a significant phenomenon in the vortex dynamics.

As well-known, the reconnection of vortices and the concurrent acoustic emission occur in a classical viscous fluid⁴. In this case, the viscosity plays an important role in the reconnection. The deduction from this phenomena is not applicable to the inviscid superfluid. The important difference between classical and quantized vortex cores is the density profile. The quantized vortex has the core where the superfluid density vanishes. On the other hand, the vortex core in an ordinary classical fluid has the finite fluid density. It is the core structure that causes the reconnection of quantized vortices even in an inviscid fluid.

The reconnection and the concurrent acoustic emission in superfluid are significantly related with the "eddy viscosity" which is a long-standing problem in superfluid physics. The superfluid turbulent state⁵ in a capillary flow induces excess temperature and pressure differences between both ends of the capillary. It is widely recognized that the temperature difference arises from the mutual friction due to the scattering of the excitations by the quantized vortex. On the other hand, the pressure difference is described phenomenologically by the eddy viscosity. The eddy viscosity works for superfluid and reduces its total momentum, but its origin has not been necessarily revealed. The reconnection and the concurrent acoustic emission reduce the energy of the quantized vortex, and then increase the kinetic energy of the superfluid including the sound waves. If the kinetic energy decays, the total energy and momentum of the superfluid

are reduced. Therefore, the reconnection and the concurrent acoustic emission may be the origin of the eddy viscosity.

Recently Leadbeater *et al.*⁶ found that a sound wave is emitted when two vortex rings reconnect. They calculate the energy of the sound wave by estimating the reduction of the vortex line length. Our works investigate the change of energy components when two vortices reconnect, following the method of Nore *et al.*⁷.

In this paper, we show the detailed process of the reconnection of quantized vortices by the numerical analysis of the GPE, and the concurrent acoustic emission. Section II describes the basic equations and the numerical method. In Sec. III, we show the acoustic emission when two anti-parallel vortices approach and disappear. This acoustic emission could be related with the Cherenkov resonance⁸. The obtained solutions are concerned with the stationary solitary waves studied by Jones and Roberts⁹. In Sec. IV, to show the detailed process of the reconnection, we analyze the motion of two vortices which are initially placed at a right angle. Section V describes the sequence of reconnections and concurrent acoustic emissions. This process resembles Feynman's cascade process¹⁰. Section VI describes the change in energy components. Considering the quantized vortex reconnection, we need to discuss whether it contradicts the Kelvin's circulation theorem that states the conservation law of the circulation in an ideal fluid, which will be described in Sec. VII. Section VIII is devoted to conclusions and discussions.

II. BASIC EQUATIONS AND NUMERICAL METHOD

The GPE is

$$i\hbar \frac{\partial \Psi(\mathbf{x})}{\partial t} = -\frac{\hbar^2}{2m} \nabla^2 \Psi(\mathbf{x}) + g |\Psi(\mathbf{x})|^2 \Psi(\mathbf{x}), \quad (1)$$

where $\Psi(\mathbf{x})$ is the macroscopic wave function, and the chemical potential μ is renormalized by the global gauge transformation $\Psi(\mathbf{x}) = \Psi'(\mathbf{x}) \exp(-i\mu t/\hbar)$. The coefficient g of the interaction is related with the s -wave scattering length a as $g = 4\pi\hbar^2 a/m$. The GPE conserves the number of particles and the total energy given by

$$N = \int d^3x |\Psi(\mathbf{x})|^2, \quad (2)$$

$$E_{\text{tot}} = \int d^3x \left(\frac{\hbar^2}{2m} |\nabla \Psi(\mathbf{x})|^2 + g |\Psi(\mathbf{x})|^4 \right), \quad (3)$$

respectively. This wave function is expressed in terms of a density and a phase by Madelung's transformation

$$\Psi(\mathbf{x}) = \sqrt{\rho(\mathbf{x})} \exp(i\theta(\mathbf{x})). \quad (4)$$

The superfluid velocity is given by $\mathbf{v}(\mathbf{x}) = \hbar \nabla \theta / m$, where m is the mass of bose particles.

The total energy E_{tot} can be decomposed as the following⁷:

$$E_{\text{tot}} = E_{\text{kin}} + E_{\text{int}} + E_{\text{q}}, \quad (5)$$

$$E_{\text{kin}} = \int d^3x \frac{\hbar^2}{2m} \left(\sqrt{\rho(\mathbf{x})} \mathbf{v}(\mathbf{x}) \right)^2, \quad (6)$$

$$E_{\text{int}} = \int d^3x g (\rho(\mathbf{x}))^2, \quad (7)$$

$$E_{\text{q}} = \int d^3x \frac{\hbar^2}{2m} \left(\nabla \sqrt{\rho(\mathbf{x})} \right)^2. \quad (8)$$

The kinetic energy E_{kin} is related with the velocity field, and E_{int} is the internal energy of the fluid. The quantum energy E_{q} comes from the gradient of the condensate, so that it is large when a vortex exists, as described later. Furthermore, in order to estimate the compressibility effects, we decompose $\sqrt{\rho} \mathbf{v}$ into $\sqrt{\rho} \mathbf{v} = (\sqrt{\rho} \mathbf{v})^i + (\sqrt{\rho} \mathbf{v})^c$ with $\nabla \cdot (\sqrt{\rho} \mathbf{v})^i = 0$. The corresponding components are named E_{kin}^i and E_{kin}^c , satisfying the relation $E_{\text{kin}} = E_{\text{kin}}^i + E_{\text{kin}}^c$. The compressible kinetic energy E_{kin}^c is directly concerned with the acoustic emission.

The numerical analysis is made for the normalized GPE. Equation (1) is reduced to

$$i \frac{\partial f}{\partial t} = -\nabla^2 f + |f|^2 f, \quad (9)$$

where $f = l^{3/2} \Psi$, $x \rightarrow x/l$, $t \rightarrow t/(2ml^2/\hbar)$, $l = 8\pi a$, $f = |f| e^{i\theta}$ and the healing length $\xi = 1/\sqrt{8\pi a n_0}$. Small perturbations around the uniform stationary solution yield the sound wave of velocity $c = \sqrt{2}$. A straight vortex is given by the stationary solution where $|f|$ increases from zero at the central core over the healing length to unity at infinity. This two dimensional solution is expressed as $f_0 = |f(r)| e^{i\phi}$ in the polar coordinates (r, ϕ) . An initial vortex configuration is determined by its core location and vorticity direction. For example, a vortex with a core at (x_0, y_0) in the direction of z axis gives $f(x, y, z) = f_0(x - x_0, y - y_0)$. The initial configuration with several vortices is given by multiplying each of the single vortex.

To numerically integrate the GPE, we use a *split step Fourier method*¹¹. There are several advantages of this method: (i) each time step is split into two segments, the first of which integrates the non-linear term in real space, and the second integrates the Laplacian operator in Fourier space, (ii) this method is second order accurate in the time interval of numerical analysis and all order in the space interval of that.

This method should take careful account of the placement of vortices. First, we use the periodic boundary condition, because it allows us to use Fast-Fourier-transformation, which saves computational times. Secondly, for example, a single vortex configuration in x - y plane is shown in Fig. 1. Although we need only

$[0, L] \times [0, L]$ region, the periodic box $[-L, L] \times [-L, L]$ is used in the actual numerical calculation so that we can prevent the phase discontinuity of the vortex. If $[0, L] \times [0, L]$ may be adopted as the periodic box, the phase discontinuity occurs at the boundary between periodic boxes. To prevent this discontinuity, the periodic box must be $[-L, L] \times [-L, L]$, and we would add anti-vortices at $(-x_0, y_0)$ and $(x_0, -y_0)$, a vortex at $(-x_0, -y_0)$. This procedure makes the phase well-defined everywhere.

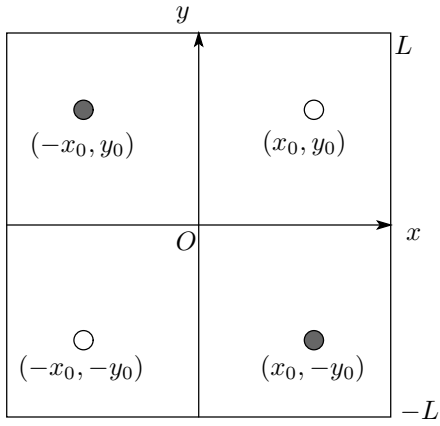


FIG. 1. Configuration of a single vortex on the $[-L, L]^2$ periodic box. When we place a vortex at (x_0, y_0) , to prevent the phase discontinuity, we add a vortex at $(-x_0, -y_0)$ and anti-vortices at $(-x_0, y_0)$ and $(x_0, -y_0)$.

In the following figures, we usually show only $[0, L]^3$ part for three-dimensional calculation and $[0, L]^2$ part for two-dimensional one. The conservation of the normalization and the total energy is confirmed numerically. These quantities are conserved in the order of 10^{-6} in all simulations.

III. ACOUSTIC EMISSION IN THE ANNIHILATION OF TWO ANTI-PARALLEL VORTICES

Consider the initial configuration where two anti-parallel vortices are placed as shown in Fig. 2(a). This is a simple and typical configuration, whose development includes the Cherenkov resonance of quantized vortices studied by Ivonin⁸ and the stationary solitary waves studied by Jones *et al.*⁹. The former is deeply concerned with the acoustic emission when two anti-parallel vortices approach and disappear. The latter shows the analytical solutions of the GPE. Jones *et al.* investigated the axisymmetric stationary solution of the GPE to obtain a continuous family consisting of two branches in the momentum-energy plane. One is a vortex ring (an anti-parallel vortex pair), and the other is a rarefaction pulse without vorticity.

As described in Appendix, two anti-parallel vortices approach each other under the periodic boundary condition. When the distance between them is reduced within a critical distance 2ξ , the velocity of two vortices becomes comparable to the sound velocity, then the local Cherenkov resonance starts and the sound waves are emitted⁸. The energy of the vortices is partly lost to the sound emission, the distance between them being reduced. These processes continue until two vortices disappear. The sound wave emitted at the moment of the annihilation has the largest amplitude in the process of the Cherenkov resonance.

In Fig. 2, the initial distance between two anti-parallel vortices, $\Delta L_0 = 1.5625\xi$, is less than 2ξ , so that they approach each other (Fig. 2(b)). Their singular lines of $|f| = 0$ overlap for a very short time and disappear.

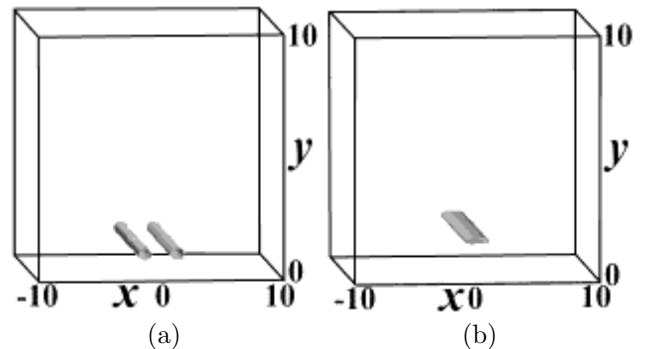


FIG. 2. Annihilation of two anti-parallel vortices, $t = 0$ (a) and $t = 0.242$ (b). The surface represents the contours of $|f| = 0.06$.

We consider the change of the condensate density $|f|$ in the process of Fig. 2. Note that it is necessary to separate carefully the effect of acoustics from that due to vortex motion. In order to reveal both the vortex motion and the acoustic emission, we show the change of $|f|$ in Fig. 3. Initially two very close depressions represent the singular cores of the vortices ((a)). They become close and overlap for a very short time and disappear ((b)). After their annihilation at $t \simeq 0.2$, the vestigial of two vortex cores becomes flattened gradually ((c)-(f)). The sound propagations are dimly shown in Fig. 3; in order to show them more clearly, Fig. 4 shows the sectional profile of the density $|f|$. After the annihilation, some wakes are found to propagate outside over the global profile; this is nothing but a sound wave. Its propagation velocity is of the same order as $c = \sqrt{2}$.

The motion of the vestigial of two vortex cores is related with the stationary solitary wave studied by Jones *et al.*⁹. We investigate the contour plots of the condensate density. These plots resemble those obtained by Jones *et al.*, although they studied the stationary solution. Our dynamical solution follows approximately the vortex solution, makes two vortex cores disappear, then follows the rarefaction pulse solution. The vestigial of the vortices correspond to the rarefaction pulse. The above sound

waves propagate over the profile of the rarefaction pulse.

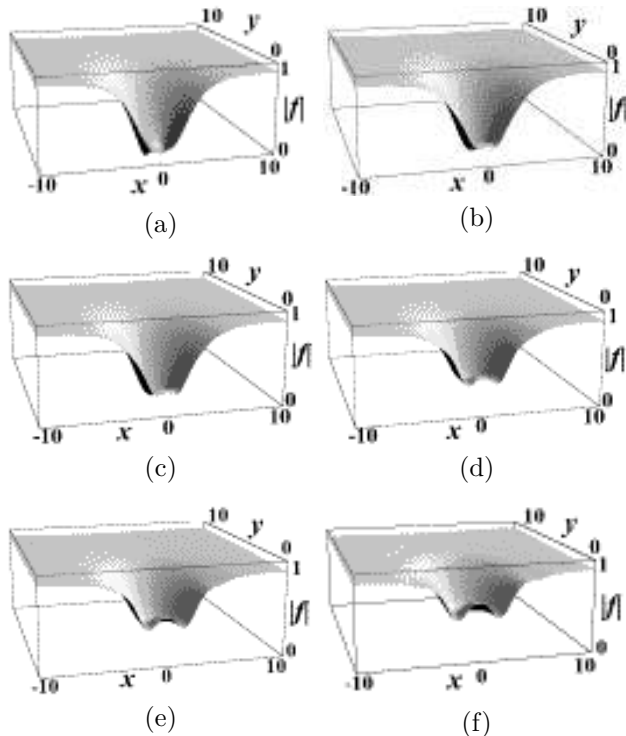


FIG. 3. Profile of $|f|$ when two anti-parallel vortices collide. The vertical axis refers to $|f|$, and the others represents the space coordinates, $t = 0$ (a), $t = 0.242$ (b), $t = 0.324$ (c), $t = 0.61$ (d), $t = 0.814$ (e), $t = 1.14$ (f). The depressions disappear(a)-(b), and the core structure are flattened gradually(c)-(f). The dimly seeable wakes are sound waves(f).

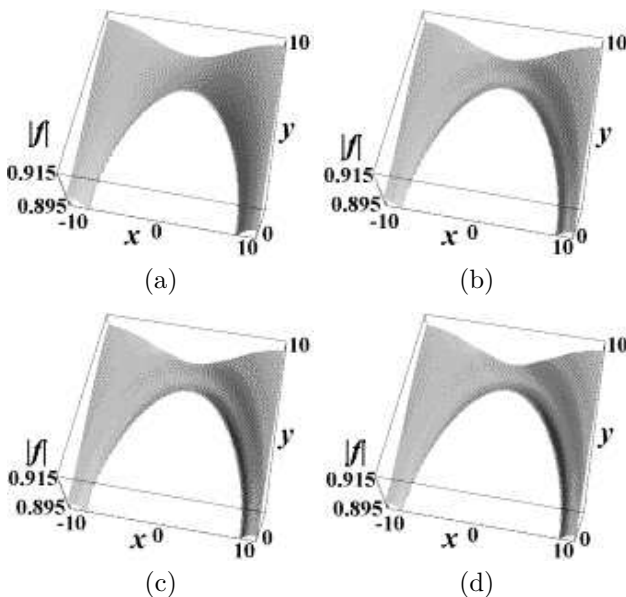


FIG. 4. Sectional profile of $|f|$. These plots show only $0.895 \leq |f| \leq 0.915$. Coordinates are the same as Fig. 3, $t = 0$ (a), $t = 1.14$ (b), $t = 1.18$ (c), $t = 1.222$ (d). Some propagated wakes are sound waves.

The change in each energy component is shown in Fig. 5. This figure does not show the internal energy component E_{int} , because it is much larger than the other components, $E_{\text{int}}/E_{\text{total}} \sim 1$. The compressible and incompressible energy increases after two vortices vanish at $t \simeq 0.2$. The increase in the compressible energy is reasonable. On the other hand, the increase in the incompressible energy may remain controversial. The quantum energy of the vortex cores is transferred irreversibly into the kinetic energy as described later.

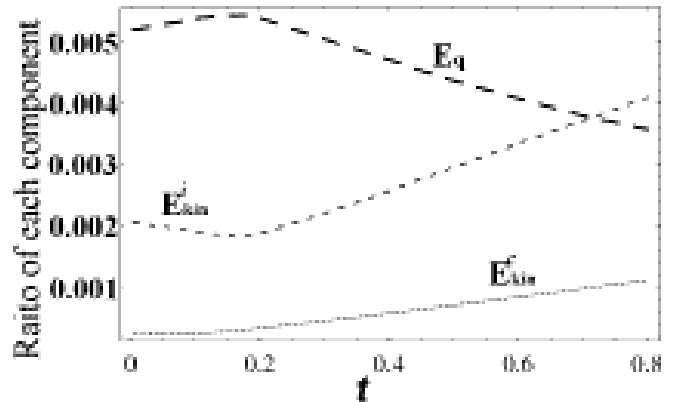


FIG. 5. Change in each energy component for the process of Fig. 2. The thick broken line, the thin broken line and the dotted line show E_q/E_{tot} , $E_{\text{kin}}^i/E_{\text{tot}}$ and $E_{\text{kin}}^c/E_{\text{tot}}$.

The sound wave affects not only the density $|f|$ but also the field of the phase θ . The vector field $\mathbf{v}_s = \nabla\theta$ in x - y planes are shown in Fig. 6. The symbols \odot and \otimes denote the singular lines with $|f| = 0$ of a vortex and an anti-vortex, respectively. Two vortices become close((a)-(c)) and disappear((d)). Before their annihilation, they become close together with the circulative field around itself. Just before the annihilation, $|\mathbf{v}_s|$ between two vortices grows very much but the density $|f|$ there is reduced. When their singular lines overlap, \mathbf{v}_s between them disappears, while the circulative field around them still remains((d)). Since the propagation speed of the event, *i.e.* “the annihilation of the singular lines”, is of the same order as c , \mathbf{v}_s far apart from the annihilation point keeps the circulative flow for a certain time((d)-(f)). After this event information comes up, the circulative flow disappears((g)-(h)). The arc shown in Fig. 6 indicates the crest of the sound wave emitted at the annihilation, which is estimated by the density propagation as shown in Fig. 3 and 4. The arc shows more clearly the disappearing processes of the circulative flow. As described before, the quantum energy of the vestigial of the singular cores are reduced and transferred into the kinetic energy. The increase in the kinetic energy results from the large velocity field near the annihilation point shown in Fig. 6(f)-(h).

Figure 7 shows the change of the vector field from the initial state

$$\delta v(x, y, t) = \frac{|\mathbf{v}(x, y, t) - \mathbf{v}(x, y, 0)|}{|\mathbf{v}(x, y, 0)|}. \quad (10)$$

These figures show the propagations of the change of the vector field, reflecting to the propagation of the sound waves as described above. The distance between two anti-parallel vortices oscillates by the acoustic emission of the Cherenkov resonance⁸, including the contribution from the vortex motion too. Although the circulative flow is slightly disarranged by the sound wave by the Cherenkov resonance for a moment, then it recovers the previous state((f)-(g)) mostly. This recovering mechanism breaks down gradually as the amplitude of the sound wave increases, eventually the circulative flow disappears after the maximum sound wave emitted at the annihilation passes by.

We investigate also the distribution of the incompressible kinetic energy density

$$e_{\text{kin}}^i(\mathbf{x}) = \left((\sqrt{\rho} \mathbf{v})^i \right)^2 \quad (11)$$

and the compressible kinetic energy density

$$e_{\text{kin}}^c(\mathbf{x}) = \left((\sqrt{\rho} \mathbf{v})^c \right)^2. \quad (12)$$

The distribution of $e_{\text{kin}}^c(\mathbf{x})$ has small peaks on the sound waves and is also spread into the whole system. On the other hand, that of $e_{\text{kin}}^i(\mathbf{x})$ has a very large peak near the vestigial of the singular cores, which contributes to the increasing in the incompressible energy in Fig. 5. Eventually, because there is no dissipative mechanism, these energy components are mixed and oscillates after that.

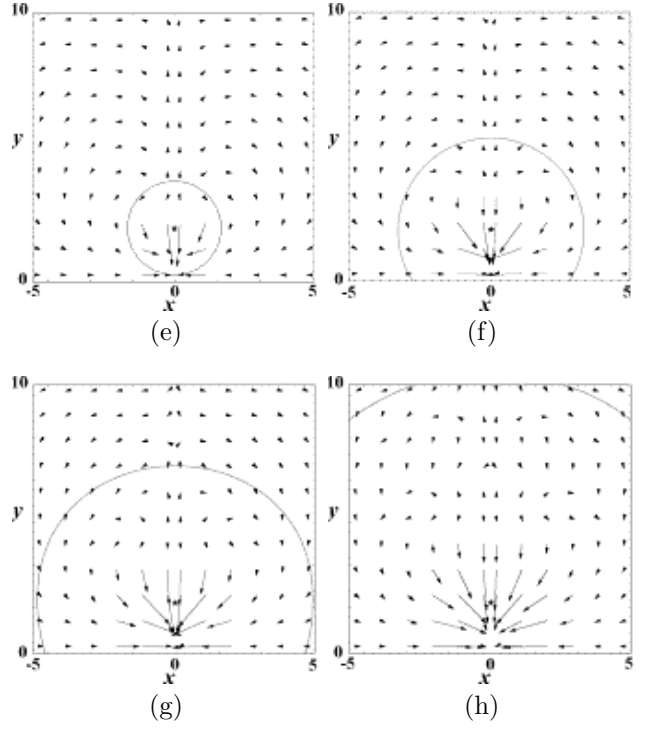
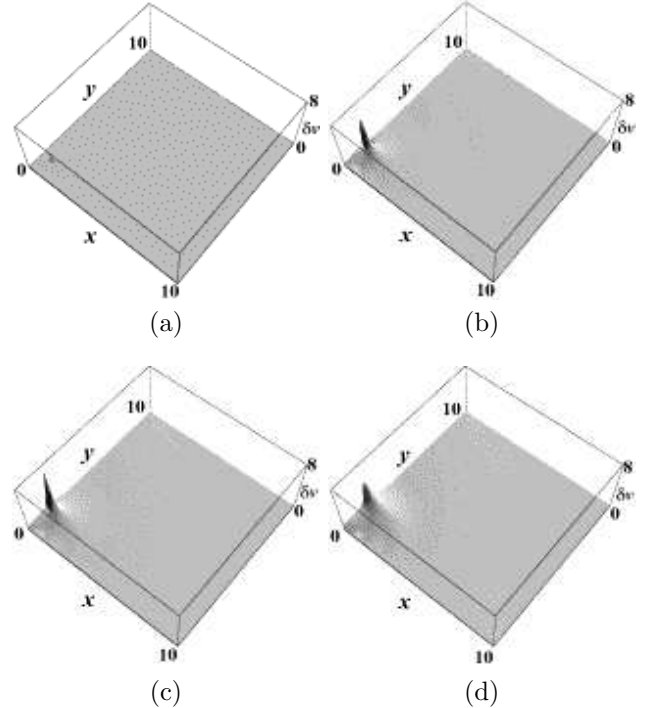
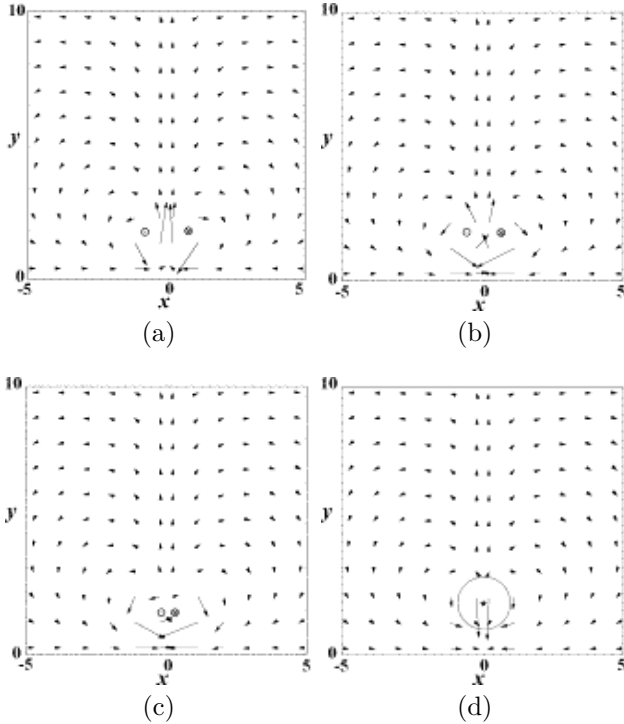


FIG. 6. Vector field $\nabla\theta$, $t=0$ (a), $t=0.14$ (b), $t=0.192$ (c), $t=0.316$ (d), $t=0.406$ (e), $t=0.61$ (f), $t=0.814$ (g), $t=1.222$ (h). The symbols \odot and \otimes denote a vortex and an anti-vortex, respectively. The vector heads denote the direction of $\nabla\theta$, and its length denotes $|\nabla\theta|$. The symbol \star shows the annihilation point, and the arc shows the crest of the sound wave emitted at the annihilation. For convenience of visualization, the vector length is stretched.



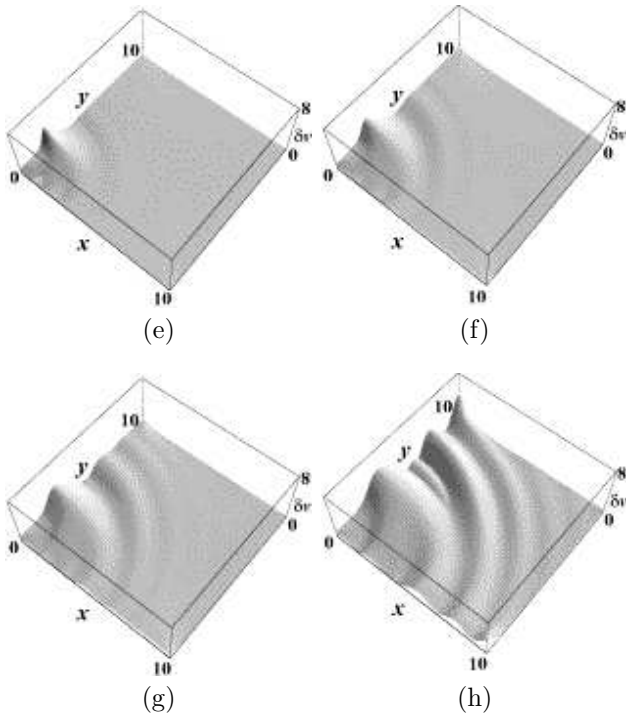


FIG. 7. Change $\delta v(x, y, t)$ of the velocity field from the initial state, $t=0$ (a), $t=0.14$ (b), $t=0.192$ (c), $t=0.316$ (d), $t=0.406$ (e), $t=0.61$ (f), $t=0.814$ (g), $t=1.222$ (h).

IV. DETAILED PROCESS OF RECONNECTION

In this section, to show the detailed processes of the reconnection, we study the three-dimensional dynamics starting from the configuration where two vortices are placed at a right angle as shown in Fig. 8(a). The grayed surfaces represents the contour of $|f| = 0.1$, which is more inside in the core than that of $|f| = \sqrt{0.3}$ calculated by Koplik *et al.*³. Two vortices cause local twists in each other((b)) so that they become locally anti-parallel at the closest point((c)) and approach each other, then reconnect((d)) and leave separately((e)-(f)). This motion is the same as that found by the filament calculation². The locally anti-parallel vortices which are closer than the critical distance become to follow the scenario of the Cherenkov resonance described in Sec. III: the anti-parallel part moves locally with the velocity comparable to the sound velocity, emits the sound wave and crosses at a point, corresponding to the two-dimensional annihilation. In order to investigate the switching of the singular core, we check the motion of the surface of $|f| = 0.03$ too as shown in Fig. 9. Two lines in Fig. 9(a)-(d) show the singular line of $|f| \simeq 0$. These lines reconnect at a point, *i.e.* the reconnecting point. Two vortices are found to reconnect at $t \sim 1.45$. The detailed processes of the reconnection are as follows: the singular cores of two vortices cross once, and keep the transient crossing for a very short time, path through each other, eventually leaving by changing their topology. The quantized vortices

reconnect without going through the classical bridge-like reconnection processes. The quantized vortex reconnection is not contrary to the Kelvin's circulation theorem, as discussed in Sec. VII.

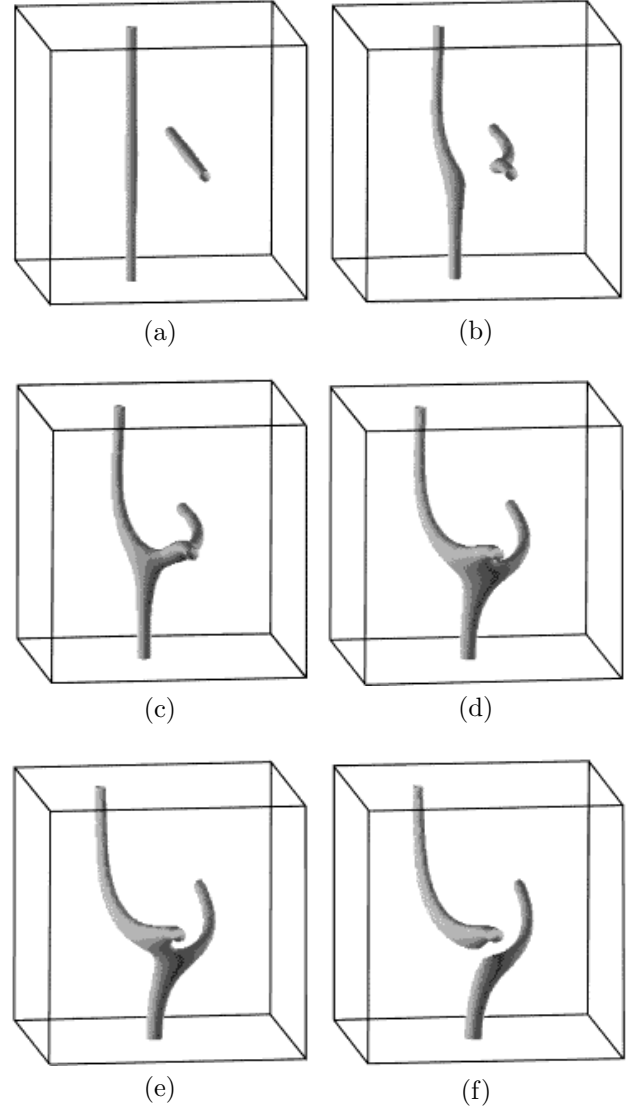


FIG. 8. Reconnection of two vortices, $t = 0$ (a), 0.816 (b), 1.224 (c), 2.448 (d), 2.856 (e), 3.06 (f). The surface represents the contour of $|f| = 0.1$. Two vortices cause local twists in each other(b) so that they become anti-parallel(c), then reconnect(d) and leave separately(e),(f).

V. SEQUENTIAL PROCESSES OF RECONNECTION AND CONCURRENT ACOUSTIC EMISSION

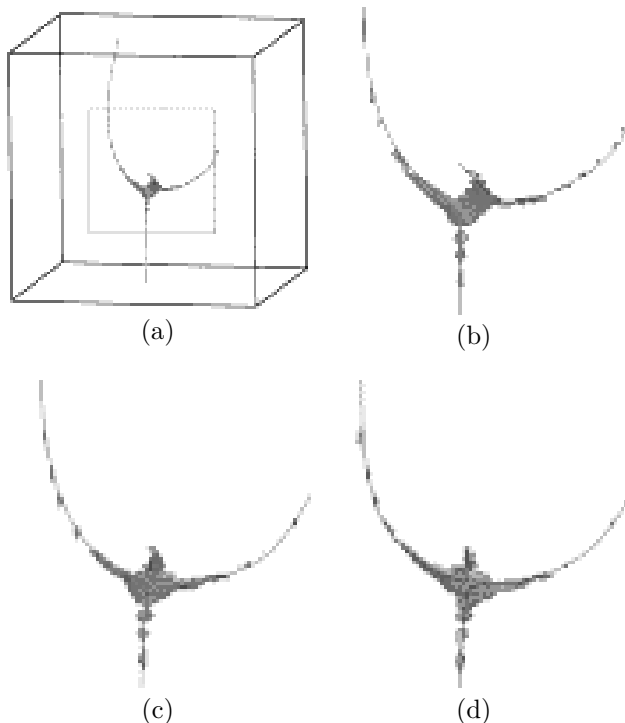


FIG. 9. More detailed reconnection process of two vortices, $t = 1.386$ (a,b), 1.428 (c), 1.46 (d). The surface represents the contour of $|f| = 0.03$. Two lines show the singular line by tracing the local minimum density less than $|f| \sim 0.06$.

Figure 10 shows the changes of the ratio of each energy component of the process of Fig. 8, which does not show E_{int} by the same reason in Sec. III. During the processes of the reconnection, E_{kin}^c and E_{kin}^i are reduced, and E_q increases. If there would be the concurrent acoustic emission, the compressible component should increase. The change of the energy components will be discussed in detail in Sec. VI.

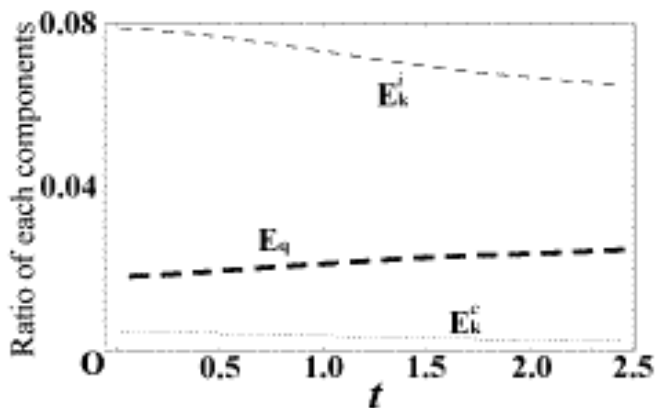


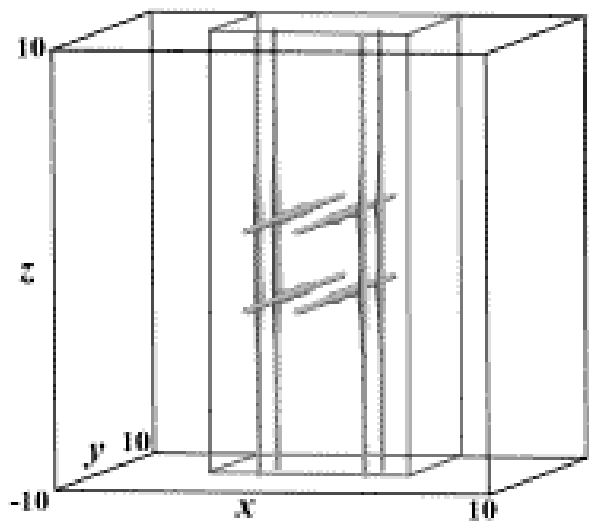
FIG. 10. Change in the energy component for the process of Fig. 8. The thick broken line, the thin broken line and the dotted line show respectively E_q/E_{tot} , $E_{\text{kin}}^i/E_{\text{tot}}$ and $E_{\text{kin}}^c/E_{\text{tot}}$.

Since the sound wave propagates over the density profile of the vortex and the vortex itself moves, we may find more easily the sound wave propagation in the region where the density of the condensate is nearly homogeneous. Thus in order to find the sound wave propagation after the reconnection of 90° vortices under the periodic boundary condition, we shift the reconnecting point toward the corner of the periodic box in this section. The initial configuration is shown in Fig. 11(a). The vortices are placed at a right angle, one has the singular core along $-\hat{z}$ direction at $(x, y) = (2.5, 1.9)$, other has that along \hat{y} direction at $(x, z) = (1.3, 1.9)$. In this configuration, we may show the density propagation enough far from the singular core.

Figure 11 shows the dynamics of two very close vortices meeting at a right angle. These figures show that the vortices are reduced to the vortex rings through the reconnections and disappear eventually. This process is the cascade process proposed by Feynman¹⁰ and revealed recently by Tsubota *et. al.*¹². For example, the vortices are broken up to smaller loops by the reconnection((d)-(e)). A small one makes self-reconnection and disappears((f)-(g)), when the energy of vortices is transferred into the kinetic energy. This is just the final stage of the cascade process. At very low temperatures, these mechanism should play a crucial role in the decay of the vortex tangle.

The changes in the ratio of each energy component are shown in Fig. 12. The figures below the horizontal axis indicate when the reconnections occur.

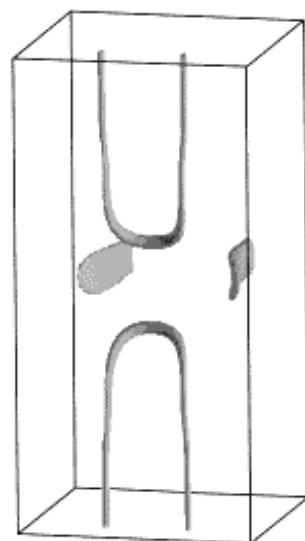
The density propagation is visible enough far from the vortex core. The dimly seeable wakes are shown in Fig. 13. In Fig. 14 which enlarges the sectional profiles of Fig. 13, the propagation of the wakes are shown properly. From the analysis of the speed of the sound wave in Sec. III, we find that the sound wave ① and ② probably comes from the reconnection ② and ③, respectively. As described before, the amplitude of the sound wave depends on how much the quantum energy is transferred into the kinetic energy, in other words, the vortex line length is lost by the reconnection. The reconnection ② is the point reconnection, while ③ is the annihilation of a small vortex ring. Although the lost line length of each two reconnection is shorter than that in Sec. III, the sound wave propagations are obviously visible. This is because the density enough far from the singular cores is about homogeneous. For example in $5 \leq x \leq 10$ and $5 \leq y \leq 10$, $|f| \sim 0.8$.



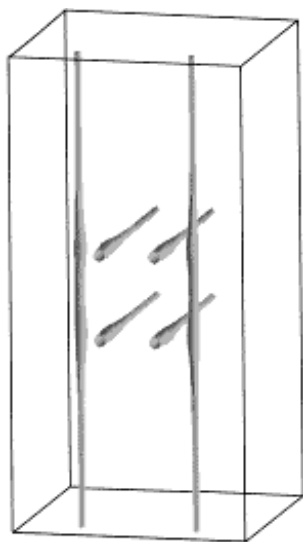
(a)



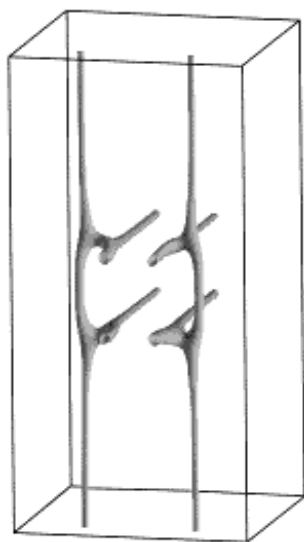
(f)



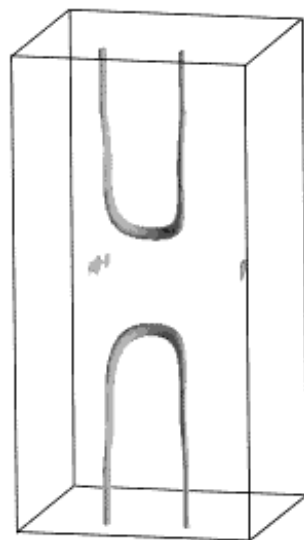
(g)



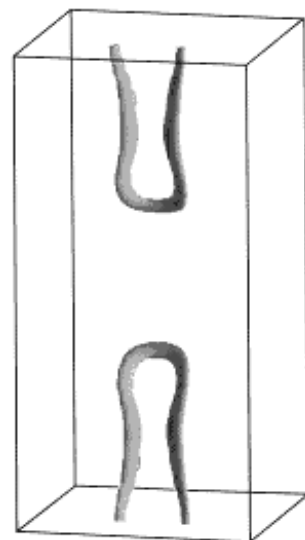
(b)



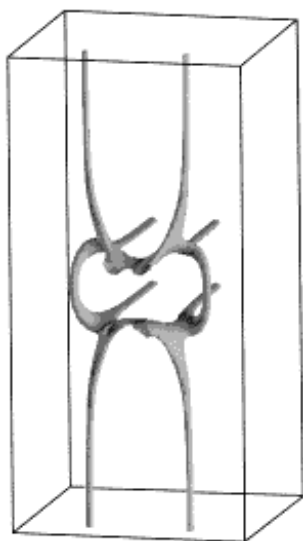
(c)



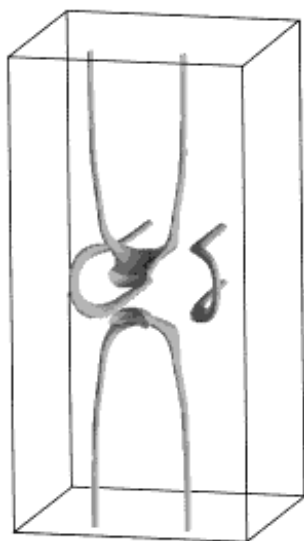
(h)



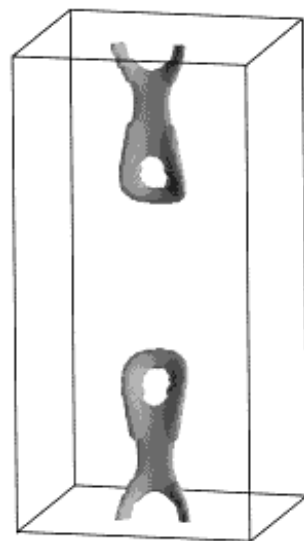
(i)



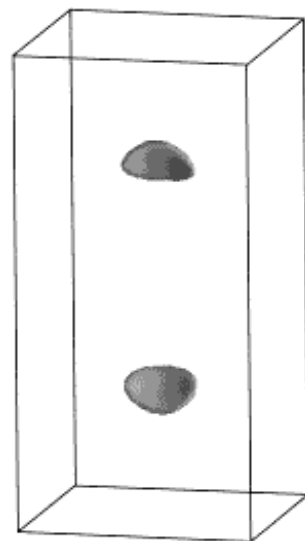
(d)



(e)



(j)



(k)

FIG. 11. Reconnections of two vortices, $t = 0.0$ (a,b), 0.182(c), 0.58(d), 0.928(e), 1.326(f), 1.794(g), 2.132(h), 3.498(i), 3.948(j), 5.172(k). The surface represents the contour of $|f| = 0.06$. The inside box of (a) indicates the region plotted in (b)-(k).

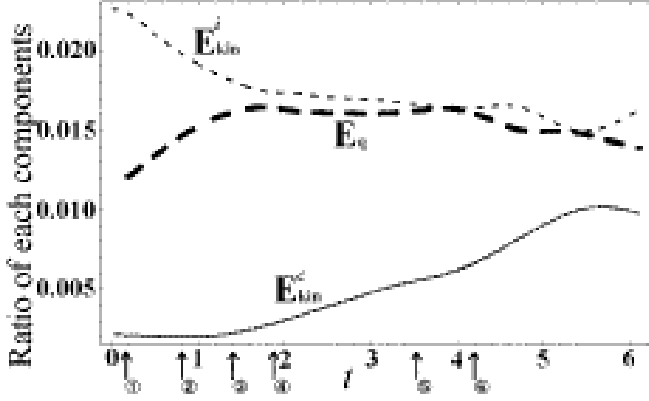


FIG. 12. Changes in each energy component of Fig. 11. The thick broken line, the thin broken line and the dotted line show respectively E_q/E_{tot} , $E_{\text{kin}}^e/E_{\text{tot}}$ and $E_{\text{kin}}^i/E_{\text{tot}}$. The numerics on the bottom show when the reconnection occurs.

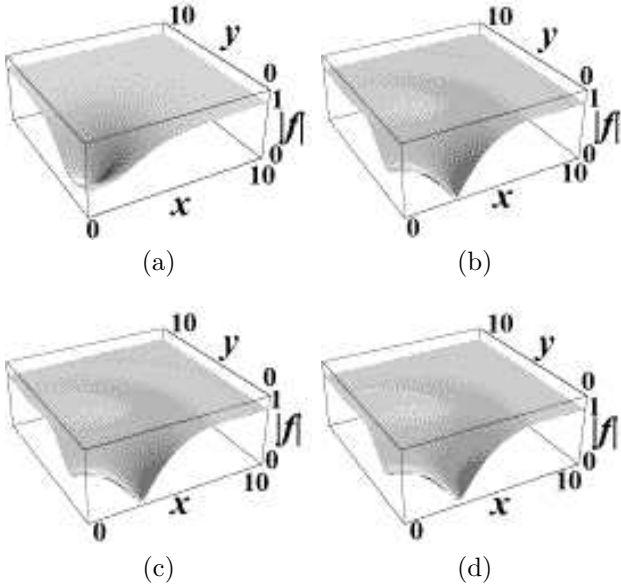


FIG. 13. Profiles of $|f|$. The vertical axis refers to $|f|$, and the others represents the space coordinates, $t = 0.0$ (a), 1.938(b), 2.04(c), 2.142(d). The dimly seeable wakes are sound waves((b)-(d)).

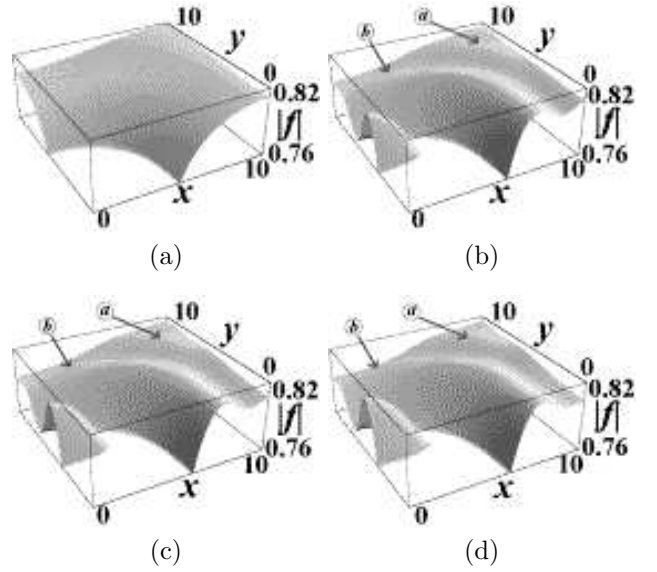


FIG. 14. Sectional profile of $|f|$. The range of $|f|$ is limited to $0.76 \leq |f| \leq 0.82$. Coordinates are the same as Fig. 13, $t = 0.0$ (a), 1.938(b), 2.04(c), 2.142(d). Some propagating wakes are sound waves.

VI. CHANGE IN THE ENERGY COMPONENTS

The comparison between Fig. 5, Fig. 10 and Fig. 12 shows some important properties on how the energy components behave. The energy is generally transferred between these three components. In fact, the changes in the components after the reconnection are roughly classified into two stages. In the first stage, E_q increases, as shown in Fig. 10, and the period $0 \leq t \leq 1.2$ of Fig. 12. Then, the vortices reconnect at points and still survive after that. The second stage is characterized by the reduction of E_q in the period $0.2 \leq t$ of Fig. 5, and the period $1.2 \leq t$ of Fig. 12: the vortex cores rather collide and disappear, than reconnect at points.

The behavior of the energy components in the first stage may be attributed at the following interaction between the vortices and the sound waves. While two vortices reconnect at a point, as shown in Fig. 8, they stretch and fat near the reconnection point because of the inter-vortex interaction. The vortices near the reconnection point move with the velocity comparable to the sound velocity. The sound waves made by the reconnection, of course, expand outside, but the above factors make the sound waves interact continuously with the vortex cores even after the reconnection. Although we do not know the detail of the interaction between quantized vortices and sound waves, this continuous interaction must make it easy that the sound waves are absorbed by the vortex cores, which increases E_q .

On the other hand, the vortex cores fade out in the second stage. Thus the quantum energy decreases, and the kinetic energy increase owing to the acoustic emission. However, $\nabla\rho$ never vanishes even after the core

structure disappears, so that the energy components are mixed and oscillate.

VII. KELVIN'S CIRCULATION THEOREM

This section comments on the conservation of the circulation $\Gamma = \oint ds \cdot \mathbf{v}$, which is called the Kelvin's circulation theorem. This theorem states that the circulation round any closed material loop is invariant in an inviscid (barotropic) fluid, and vortices are never born, die and reconnect. It seems that the theorem does not allow the above reconnection of quantized vortex. Then, we have to consider two problems: (i) is this theorem applicable to the superfluid dynamics derived from the GPE? (ii) what happens to the material loops when quantized vortices reconnect? Equation (9) yields the equation of motion for superflow:

$$\frac{D\mathbf{v}}{Dt} = \nabla \left(\frac{\nabla^2 |f|}{|f|} \right) = \nabla w, \quad (13)$$

where $D/Dt \equiv \partial/\partial t + \mathbf{v} \cdot \text{grad}$. By differentiating Γ with respect to t , we obtain

$$\frac{D\Gamma}{Dt} = \oint ds \cdot \nabla \left(w + \frac{\mathbf{v}^2}{2} \right). \quad (14)$$

Therefore $\Gamma = \text{const.}$ if w is well-defined on the material loop along which Γ is defined (i). When two vortices are about to reconnect, almost all material loops are carried away from the merger region by the flow (Fig. 15(a)) (ii). The loop just going through the reconnecting point breaks this theorem because w is not well-defined owing to $|f| = 0$, thus leading to the reconnection (Fig. 15(b)). This is the peculiar situation in superfluid. Thus the reconnection of quantized vortices is not contradictory to the Kelvin's circulation theorem.

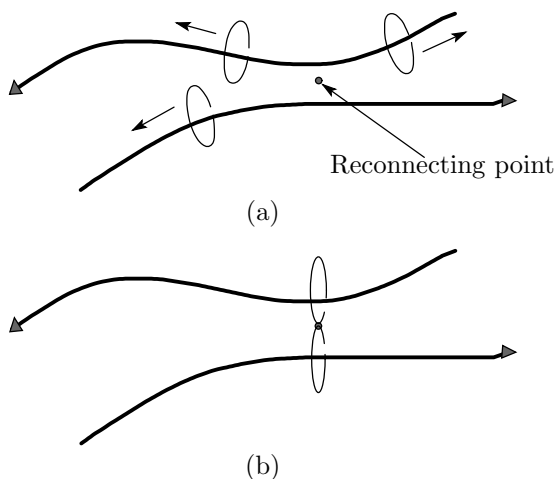


FIG. 15. Motion of the material loops when two vortices reconnect. (a): most loops are carried away from the merger region by the flow. (b): the Kelvin's circulation theorem breaks on the loops going through the reconnecting point.

VIII. CONCLUSIONS AND DISCUSSIONS

We studied numerically the reconnection of quantized vortices and the concurrent acoustic emission by the analysis of the GPE. The energy components are analyzed for every dynamics.

When two anti-parallel vortices are close within a critical distance which is twice the healing length, they move with the velocity comparable to the sound velocity, emit the sound waves and disappear; this phenomena is closely concerned with the Cherenkov resonance. The propagation of the sound waves not only appears in the density profile of the wave function but also affects the phase field; they destroy the circulative velocity field that belonged to the vortices originally.

Two straight vortices meeting initially at a right angle follow the scenario similar to the vortex filaments, thus reconnecting. The singular lines of $|f| = 0$ cross once at a point, switch their topology instantly and leave separately. This reconnection is not contradictory to the Kelvin's circulation theorem, because the potential of the superflow field becomes undefined at the reconnection point.

Two close straight vortices meeting at a right angle, under the periodic boundary condition, follow a series of reconnection, breaking up to smaller vortex loops. Eventually these loops disappear through self-reconnections with the acoustic emission. The process transforms irreversibly the quantum energy of the vortex cores to the kinetic energy. This may represent the final stage of the vortex cascade process.

The change in energy components depends on how the vortices reconnect. When vortices survive still after reconnections, the emitted sound waves interact continuously with the vortex cores. Then sound waves are absorbed by the vortex cores, which increases the quantum energy. On the other hand, when vortex loops disappear through reconnections, the quantum energy is transferred into the kinetic energy with the acoustic emission.

Throughout this work, it remains unresolved how sound waves interact with quantized vortices; they may stretch and fat the vortex cores or excite the Kelvin waves¹³. More detailed studies of the interaction are being carried out.

ACKNOWLEDGEMENT

We are grateful to W. F. Vinen, M. E. Brachet, C. S. Adams, T. Araki and T. Tatsuta for useful discussion.

APPENDIX: MOTION OF ANTI-PARALLEL VORTICES BY THE FILAMENT FORMULATION

This appendix describes the motion of the vortices initially placed as shown in Fig. 16 by the vortex filament

formulation¹⁴. The velocity field generated by a vortex whose singular core is at the origin is given by

$$v_s = \frac{\kappa}{2\pi r}, \quad (\text{A1})$$

where κ is the quantized circulation. The motion of equation of the vortex 1 is given by

$$\dot{\mathbf{s}} = \mathbf{v}_1 = \mathbf{v}_{21} + \mathbf{v}_{31} + \mathbf{v}_{41}, \quad (\text{A2})$$

where $\mathbf{s} = (x, y)$, and \mathbf{v}_{21} , \mathbf{v}_{31} and \mathbf{v}_{41} are the velocity field at the position of vortex 1 generated by the vortex 2, 3 and 4, respectively. Each velocity are given by

$$\mathbf{v}_{21} = \frac{\kappa}{2\pi} \left(0, \frac{1}{2x} \right), \quad (\text{A3})$$

$$\mathbf{v}_{31} = \frac{\kappa}{2\pi} \frac{1}{2r} (\sin \theta, -\cos \theta), \quad (\text{A4})$$

$$\mathbf{v}_{41} = \frac{\kappa}{2\pi} \left(-\frac{1}{2y}, 0 \right). \quad (\text{A5})$$

Therefore, the dimensionless form of the equations of motion are

$$\dot{x} = -\frac{1}{y} + \frac{y}{x^2 + y^2}, \quad \dot{y} = \frac{1}{x} - \frac{x}{x^2 + y^2}, \quad (\text{A6})$$

where $t \cdot \kappa/2\pi \rightarrow t$. These equations can be rewritten in term of the polar coordinates:

$$\dot{r} = -\frac{2}{r} \cot 2\theta, \quad \dot{\theta} = \frac{1}{r^2} > 0. \quad (\text{A7})$$

Therefore

$$\frac{dr}{d\theta} = -2r \cot 2\theta. \quad (\text{A8})$$

For example the vortex 1 is initially placed at $(r, \theta) = (r_0, \pi/4)$,

$$\frac{r_0}{r} = \sin 2\theta. \quad (\text{A9})$$

This equation can be rewritten in term of the Cartesian coordinates:

$$y^2 = \frac{\frac{r_0^2}{4}}{x^2 - \frac{r_0^2}{4}} \quad (\text{A10})$$

This solution means that the vortex pair above x axis moves upward and approaches each other down to a certain distance determined by the initial configuration as shown in Fig. 16 (b), *i.e.* $\Delta L = r_0$.

If ΔL becomes comparable to the healing length, the vortex filament formulation becomes not available, leading to the pair annihilation as described in the text.

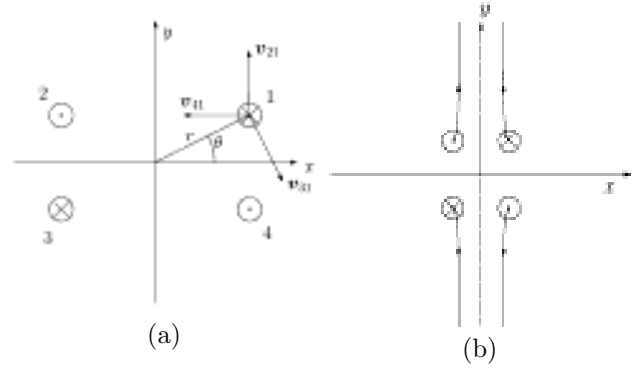


FIG. 16. (a) The initial configuration of Sec.III. The \odot and \otimes symbols indicate a vortex and an anti-vortex. (b) The trajectories of each vortex. the vortex pair above x axis moves upward and approaches each other down to a certain distance.

- ¹ R. J. Donnelly, *Quantized Vortices in Helium II*, Cambridge Studies in Low Temperature Physics Vol. 3, Cambridge University Press.
- ² K.W.Schwarz, *Phys. Rev. B* **31**, 5782(1985); *ibid* **38** 2398(1988)
- ³ J.Koplik and H.Levine, *Phys. Rev. Lett.* **71**, 1375(1993); *ibid* **76**, 4745(1996).
- ⁴ O.Inoue and Y.Hattori, *Proc. IUTAM Symposium on Dynamics of Slender Vortices*(Kluwer Academic Publishers), 361(1997).
- ⁵ J.T.Tough, in *Progress in Low Temperature Physics*, edited by D.F.Brewer(North-Holland, Ameterdam, 1982), Vol.VIII, p.134.
- ⁶ M. Leadbeater, T. Winiecki, D. C. Samuels, C. F. Barenghi and C. S. Adams, cond-mat/0009060
- ⁷ C. Nore, M. Abid and M. E. Brachet, *Phys. Fluids* **9**, 2644(1997).
- ⁸ I. A. Ivonin, *Sov. Phys. JETP* **85**, 1233(1997)
- ⁹ C. F. Jones and P. H. Roberts, *J. Phys. A: Math. Gen.* **15**, 2599(1982)
- ¹⁰ R.P.Feynman, in *Progress in Low Temperature Physics*, edited by C.J.Gorter(North-Holland, Ameterdam, 1955), Vol.I, p.17.
- ¹¹ T. Taha and M. Ablowitz, *J. Comput. Phys.* **55**, 203(1984)
- ¹² M. Tsubota, T.Araki and S.K.Nemirovskii, *Phys. Rev. B* **62** 11751(2000)
- ¹³ W.F.Vinen, *Phys. Rev. B* **61**, 1410(2000).
- ¹⁴ H. Lamb, *Hydrodynamics* 6th edition, Cambridge University Press, 1932